Syntheses, Structures, and Electrochemistry of Polynuclear CuI, AgI, and PtII Complexes Bearing Ferrocenyl Group

ARTICLE *in* ORGANOMETALLICS · MARCH 2002

Impact Factor: 4.13 · DOI: 10.1021/om010998m

5 AUTHORS, INCLUDING:

Jianguo Wu
Yale University
23 PUBLICATIONS **440** CITATIONS

SEE PROFILE

Syntheses, Structures, and Electrochemistry of Polynuclear Cu^{I}, Ag^{I}, and Pt^{II} Complexes Bearing Ferrocenyl Group

John H. K. Yip,*,† Jianguo Wu,† Kwok-Yin Wong,*,‡ Kin-Wai Yeung,‡ and Jagadese J. Vittal†

Department of Chemistry, The National University of Singapore, 10 Kent Ridge Crescent, Singapore, 119260, and Department of Applied Biology and Chemical Technology, Hong Kong Polytechnic University, Hunghom, Kowloon, Hong Kong, People's Republic of China

Received November 19, 2001

Three polynuclear complexes, $[Pt^{II}_2(dppm)_2(\mu\text{-}\eta^1\text{:}\eta^1\text{-HC=CFc})Cl_2]$ (**1**), $[Ag^{I}_3(dppm)_3(\mu_3\text{-}\eta^1\text{-C≡CFc})]\cdot 2CF_3SO_3$ (**2**$\cdot 2CF_3SO_3$), and $[Cu^{I}_3(dppm)_3(\mu_3\text{-}\eta^1\text{-C≡CFc})_2]\cdot PF_6$ (**3**$\cdot PF_6$), were synthesized and characterized using single-crystal X-ray diffraction, UV−vis spectroscopy, and voltammetry (dppm = bis(diphenylphosphino)methane; Fc = ferrocenyl). Compound **1** is an A-frame complex in which two Pt^{II} ions are bridged by two dppm and one ethynylferrocene. Both **2**$\cdot 2CF_3SO_3$ and **3**$\cdot PF_6$ are composed of trimetallic Ag^{I}_3 and Cu^{I}_3 cores bridged by three dppm and capped with one and two ferrocenylacetylides, respectively. All complexes exhibit reversible Fc oxidation in their cyclic voltammograms (CV), ranging from -48 ± 10 to 235 ± 10 mV vs $Ag/AgNO_3$ (0.1 M). The reduction potential difference between silver and copper complexes is mostly due to intramoleuclar electrostatic interactions. A weak intervalence charge-transfer transition at 1250 nm arising from the mixed-valence $\mathbf{3}^{2+}$ is observed in the solution near-infrared absorption spectrum of a mixture of **3**$\cdot PF_6$ and ferrocenium hexafluorophosphate (Cp_2FePF_6). Cyclic and differential pulse volatmmograms of **3**$\cdot PF_6$ show two reversible Fc oxidations separated by 110 ± 14 mV, giving a comproportionation constant K_c of 77 ± 30. The stability of the mixed-valence complex $\mathbf{3}^{2+}$ arises mainly from the reduction of electrostatic repulsion and statistical distribution.

Introduction

Electron transfer is pivotal to the functioning of many biological and artificial molecular devices.[1] Essential components of these systems include an electron donor (D) and an acceptor (A) connected by a set of bonds, commonly known as bridge or spacer. The bridge plays a crucial role in electron transfer, as its length, electronic structure, and composition affect the electronic communication between D and A. In his pioneer work, Taube examined the electron delocalization in mixed-valence $Ru^{II}-L-Ru^{III}$ compounds in which the metal centers are linked by various organic bridges L.[2−5] The extent of electron delocalization in the mixed-valence compounds is reflected by the comproportionation constant (K_c) obtained from electrochemical measurements or redox titration[5] and the electronic coupling parameter H_{AB} calculated from the near-infrared (NIR) absorption energy and intensity.[6] Since then, there have been a lot of experimental[7−20] and theoretical[6,21−23] investigations on the effect of bridge on electronic interactions between metal centers. In the recent search for molecular

* Corresponding authors. Fax: 65-7791691. E-mail: chmyiphk@nus.edu.sg.
† The National University of Singapore.
‡ Hong Kong Polytechnic University.

(1) (a) Marcus, R. A. *Angew. Chem., Int. Ed. Engl.* **1993**, *32*, 111. (b) Ballardini, R.; Balzani, V.; Credi, A.; Gandolfi, M. T.; Venturi, M. *Acc. Chem. Res.* **2001**, *36*, 445.
(2) Creutz, C.; Taube, H. *J. Am. Chem. Soc.* **1973**, *95*, 1086.
(3) Taube, H. *Electron-Transfer Reactions of Complexes in Solution*; Academic Press: New York, 1970.
(4) Richardson, D. E.; Taube, H. *Coord. Chem. Rev.* **1984**, *60*, 107.
(5) Creutz, C. In *Prog. Inorg. Chem.* Lippard, S. J., Ed.; Wiley: New York 1983; Vol. 30, 1.
(6) Hush, N. S. *Prog. Inorg. Chem.* **1967**, *8*, 391.
(7) For recent reviews in mixed-valence compounds see: (a) Astruc, D. *Acc. Chem. Res.* **1997**, *30*, 383. (b) McCleverty, J. A.; Ward, M. D. *Acc. Chem. Res.* **1998**, *31*, 842. (c) Kaim, W.; Klein, A. Glöckle, M. *Acc. Chem. Res.* **2000**, *33*, 755. (d) Barlow, S.; O'Hara, D. *Chem. Rev.* **1997**, *97*, 637.
(8) Glöckle, M.; Kaim, W.; Fiedler, J. *Organometallics* **1998**, *17*, 4923.
(9) Atwood, C. P.; Geiger, W. E. *J. Am. Chem. Soc.* **2000**, *122*, 5477.
(10) Glöckle, M.; Kaim, W.; Katz, N. E.; Posse, M. G.; Cutin, E. H.; Fiedler, J. *Inorg. Chem.* **1999**, *38*, 3270.
(11) Ribou, A. C.; Launay, J.-P.; Sachtleben, M. L.; Li, H.; Spangler, C. W. *Inorg. Chem.* **1996**, *35*, 3735.
(12) Nelsen, S. F.; Ismagilov, R. F.; Powell, D. R. *J. Am. Chem. Soc.* **1998**, *120*, 1924.
(13) Cargill Thompson, A. M. W.; Gatteschi, D.; McCleverty, J. A.; Navas, J. A.; Rentschler, E.; Ward, M. D. *Inorg. Chem.* **1996**, *35*, 2701.
(14) Dembinski, R.; Bartik, T.; Bartik, B.; Jaeger, M.; Gladysz, J. A. *J. Am. Chem. Soc.* **2000**, *122*, 810.
(15) Bruce, M. I.; Low, P. J.; Costuas, K.; Halet, J.-F.; Best, S. P.; Heath, G. A. *J. Am. Chem. Soc.* **2000**, *122*, 1949.
(16) Morrison, W. H., Jr.; Hendrickson, D. N. *Inorg. Chem.* **1975**, *14*, 2331.
(17) Rittinger, S.; Buchholz, D.; Delville-Desbois, M. H.; Linares, J.; Varret, F.; Boese, R.; Zsolnai, L.; Huttner, G.; Astruc, D. *Organometallics* **1992**, *11*, 1454.
(18) Dong, T. Y.; Chang, C. K.; Lee, S. H.; Lai, L. L.; Chiang, M. Y. N.; Lin, K. J. *Organometallics* **1997**, *16*, 5816.
(19) Barlow, S.; Murphy, V. J.; Evan, J. S. O.; O'Hara, D. *Organometallics* **1995**, *14*, 3461.
(20) Justin Thomas, K. R.; Lin, J. T.; Wen, Y. S. *Organometallics* **2000**, *19*, 1008.
(21) Crutchley, R. J. *Adv. Inorg. Chem.* **1994**, *41*, 273.
(22) Hush, N. S. *Coord. Chem. Rev.* **1985**, *64*, 135.
(23) Patoux, C.; Coudret, C.; Launay, J.-P.; Joachim, C.; Gourdon, A. *Inorg. Chem.* **1997**, *36*, 5037.

10.1021/om010998m CCC: $22.00
Publication on Web 03/13/2002

wires,[25−31] attention has been drawn to donor−acceptor compounds that contain metal (M) as part of the bridge (D−M−A).[32−42] Examples of D−M−A compounds are *trans*-[$Pt^{II}(PPh_3)_2(C{\equiv}CFc)_2$][35,36] (Fc = ferrocenyl) and *trans*-[$Ru^{II}(dppm)_2(C{\equiv}CFc)_2$].[32−34] Studies showed that the nature of the transition metal and its electronic properties play a key role in the electronic coupling and hence electron delocalization in these systems. For example, *trans*-[$Ru^{II}(dppm)_2(C{\equiv}CFc)_2]^+$ [32−34] was found to be a Robin-Day class II[43] mixed-valence system, and the degree of electronic coupling is dependent on the ancillary ligands.[34] On the other hand, the analogous Pt complex *trans*-[$Pt^{II}(PMePh_2)_2(C{\equiv}CFc)_2$] shows weak electronic coupling ($K_c = 80$).[36] In addition, it has been shown that the extent of electron delocalization in a series of [LFeMFeL]$^{n+}$ complexes can be influenced by changing the central metal M (L = 1,4,7-tris(4-*tert*-butyl-2-mercaptobenzyl)-1,4,7-triazacyclononane, M = Fe, Co, and Cr).[37]

So far most of the studies in this area focused on D−M−A systems which contain a single metal in the spacer, and relatively limited work has been carried out to investigate how polymetallic centers mediate electron delocalization, despite the wide occurrence of metal clusters in electron-transfer proteins.[44] One of the examples in this area is the electrochemical study of an Fe_4S_4 cluster bonded with redox-active $[W(CO)_5CN]^-$.[45] In addition, electronic communication between Fc groups through cobalt−carbonyl clusters[46−48] and 1,12-*para*-carborane $CB_{10}H_{10}C$[48] was examined. Related studies include recent work on charge delocalization in Fc-C≡C−C≡C−Fc modified with the Os_3CO_9 cluster.[49,50] Herein we describe the synthetic, structural, and electrochemical studies of the trinuclear Cu^I_3 and Ag^I_3 and binuclear Pt^{II}_2 complexes which contain one or two redox-active Fc groups (Scheme 1). Of particular interest to us are (i) the nature of the coordinated ethynylferrocene in **1**, (ii) the electronic interaction between the trimetallic clusters and the Fc group in $\mathbf{2}^{2+}$ and $\mathbf{3}^+$, and (iii) the electronic communication (if there is any) across the $C_2-Cu_3-C_2$ bridge in the one-electron-oxidized $\mathbf{3}^{2+}$. Recently, trinuclear copper−acetylides $[Cu_3(P{\wedge}P)_3(\mu_3\text{-}\eta^1\text{-}C{\equiv}CR)_2]^+$ (P∧P = bridging diphosphine and R = alkyl/aryl)[51−57] have drawn considerable attention mostly because of their photophysical and photochemical properties.[54−57] In view of the claimed potentials of the compounds in serving as molecular devices, it is essential to understand the nature of the Cu^I_3-acetylide, especially their ability to mediate electron delocalization. To address this question, we synthesized the model compound $[Cu_3(dppm)_3(\mu_3\text{-}\eta^1\text{-}C{\equiv}CFc)_2]\cdot PF_6$ (**3**·PF_6), which contains two terminal ferrocenylacetylides ($FcC{\equiv}C^-$) across a Cu^I_3 core. The "conductivity" of the trinuclear Cu^I_3 core was examined by using cyclic and differential pulse voltammetry.

Scheme 1

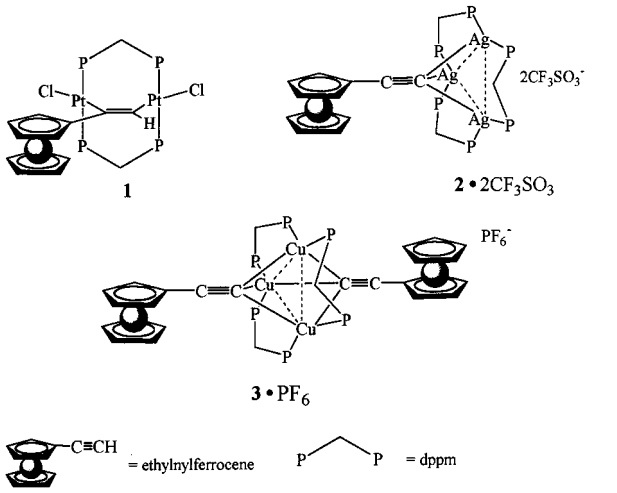

Experimental Section

General Methods. All syntheses were carried out using standard Schlenck techniques. $AgCF_3SO_3$ and dppm were obtained from Aldrich and used as received. All solvents used in syntheses and electrochemical measurements were purified according to the literature methods. The supporting electrolyte

(24) Paul, F.; Lapinte, C. *Coord. Chem. Rev.* **1998**, *180*, 431.
(25) Paul, F.; Meyer, W. E.; Toupet, L.; Jiao, H. J.; Gladysz, J. A.; Lapinte, C. *J. Am. Chem. Soc.* **2000**, *122*, 9405.
(26) Rigaut, S.; Le Pichon, L.; Daran, J. C.; Touchard, D.; Dixneuf, P. H. *J. Chem. Soc., Chem. Commun.* **2001**, 1206.
(27) Long, N. J.; Martin, A. J.; Vilar, R.; White, A. J. P.; Williams, D. J.; Younus, M. *Organometallics* **1999**, *18*, 4261.
(28) Xue, W.-M.; Kühn, F. E. *Eur. J. Inorg. Chem.* **2001**. 2041.
(29) Zhu, Y. B.; Wolf, M. O. *J. Am. Chem. Soc.* **2000**, *122*, 10121.
(30) Hradsky, A.; Bildstein, B.; Schuler, N.; Schottenberger, H.; Jaitner, P.; Ongania, K.-H.; Wurst, K.; Launay, J.-P. *Organometallics* **1997**, *16*, 392.
(31) Ward, M. D. *Chem. Soc. Rev.* **1995**, 121.
(32) Colbert, M. C. B.; Lewis, J.; Long, N. J.; Raithby, P. R.; White, A. J. P.; Williams, D. J. *J. Chem. Soc., Dalton Trans.* **1997**, 99.
(33) Zhu, Y.; Clot, O.; Wolf, M. O.; Yap, G. P. A. *J. Am. Chem. Soc.* **1998**, *120*, 1812.
(34) Jones, N. D.; Wolf, M. O.; Giaquinta, D. M. *Organometallics* **1997**, *16*, 1352.
(35) Osella, D.; Gambino, O.; Nervi, C.; Ravera, M.; Russo, M. V.; Infante, G. *Inorg. Chim. Acta* **1994**, *225*, 35.
(36) Osella, D.; Gobetto, R.; Nervi, C.; Ravera, M.; D'Amato, R.; Russo, M. V. *Inorg. Chem. Commun.* **1998**, *1*, 239.
(37) Glaser, T.; Beissel, T.; Bill, E.; Weyhermüller, T.; Schünemann, V.; Meyer-Klaucke, W.; Trautwein, A. X.; Wieghardt, K. *J. Am. Chem. Soc.* **1999**, *121*, 2193.
(38) Back, S.; Rheinwald, G.; Lang, H. *Organometallics* **1999**; *18*, 4119.
(39) Lebreton, C.; Touchard, D.; Pichon, L. L.; Daridor, A.; Toupet, L.; Dixneuf, P. H. *Inorg. Chim. Acta* **1998**, *272*, 188.
(40) Lavastre, O.; Plass, J.; Bachmann, P.; Guesmi, S.; Moinet, C.; Dixneuf, P. H. *Organometallics* **1997**, *16*, 184.
(41) Hore, L. A., McAdam, C. J.; Kerr, J. L.; Duffy, N. W.; Robinson, B. H.; Simpson, J. *Organometallics* **2000**, *19*, 5039.
(42) McAdam, C. J.; Brunton, J. J.; Robinson, B. H.; Simpson, J. *J. Chem. Soc., Dalton Trans.* **1999**, 2487.
(43) Robin, M. B.; Day, P. *Adv. Inorg. Chem. Radiochem.* **1967**, *10*, 247.
(44) Beinert, H. *J. Biol. Inorg. Chem.* **2000**, *5*, 2.
(45) Zhu, N.; Pebler, J.; Vahrenkamp, H. *Angew. Chem., Int. Ed. Engl.* **1996**, *35*, 894.
(46) McAdam, C. J.; Duffy, N. W.; Robinson, B. H.; Simpson, J. *Organometallics* **1996**, *15*, 3935.
(47) Osella, D.; Nervi, C.; Ravera, M.; Duffy, N. W.; McAdam, C. J.; Robinson, B. H.; Simpson, J. *Inorg. Chim. Acta* **1996**, *247*, 99
(48) Fox, M. A.; Paterson, M. A. J.; Nervi, C.; Galeotti, F.; Puschmann, H.; Howard, J. A. K.; Low, P. J. *J. Chem. Soc., Chem. Commun.* **2001**, 1610.
(49) Adams, R. D.; Qu, B. *Organometallics* **2000**, *19*, 2411.
(50) Adams, R. D.; Qu, B. *Organometallics* **2000**, *19*, 4090.
(51) Gamasa, M. P.; Gimeno, J.; Lastra, E.; Aguirre, A.; García-Granda, S. *J. Organomet. Chem.* **1989**, *378*, C11.
(52) Diez, J.; Gamasa, M. P.; Gimeno, J.; Aguirre, A.; García-Granda, S. *Organometallics* **1991**, *10*, 380.
(53) Diez, J.; Gamasa, M. P.; Gimeno, J.; Aguirre, A.; García-Granda, S. *Organometallics* **1993**, *12*, 2213.
(54) Yam, V. W. W.; Lee, W. K.; Cheung, K. K.; Crystall, B.; Phillips, D. *J. Chem. Soc., Dalton Trans.* **1996**, 3283.
(55) Yam, V. W. W.; Fung, W. K. M.; Wong, M. T. *Organometallics* **1997**, *16*, 1772.
(56) Yam, V. W. W.; Fung, W. K. M.; Cheung, K. K. *Organometallics* **1998**, *17*, 3293.
(57) Yam, V. W. W.; Fung, W. K. M.; Wong, K. M. C.; Lau, V. C. Y.; Cheung, K. K. *J. Chem. Soc., Chem. Commun.* **1998**, 777.

tetra-*n*-butylammonium hexafluorophophate (TBAH) obtained from Aldrich was recrystallized from ethanol and dried at 100 °C for 24 h before use. Ethynylferrocene,[58] $[Pt_2(dppm)_2Cl_2]$,[59] and Cp_2FePF_6[60] were prepared according to reported procedures. $Cu_2(dppm)_2(MeCN)_2(PF_6)_2$ and $Ag_2(dppm)_2(CF_3SO_3)_2$ were synthesized by reacting dppm with 1 equiv of $Cu(CH_3CN)_4PF_6$ and $AgCF_3SO_3$ in acetonitrile, respectively.

Physical Measurements. The UV−vis absorption spectra of the complexes were recorded on a Hewlett-Packard HP8452A diode array spectrophotometer. ^1H and ^{31}P NMR spectra were recorded at 25 °C on a Bruker ACF 300 spectrometer. Elemental analyses of the complexes were carried out in the microanalysis laboratory in the Department of Chemistry, the National University of Singapore. Solution infrared spectra of the complexes were recorded on a Bio-Rad TFS 156 spectrometer. Near-infrared absorption spectra were recorded on a Perkin-Elmer Lambda 900 UV/vis/NIR spectrometer. Acetonitrile and dichloromethane used for the voltammetric measurements were distilled over CaH_2 and P_2O_5, respectively. A Bioanalytical Systems (BAS) model 100W electrochemical analyzer was used in all electrochemical measurements. Tetra-*n*-butylammonium hexafluorophosphate (0.1 M) was used as the supporting electrolyte unless otherwise stated. Cyclic voltammetry and differential pulse voltammetry were performed in a conventional two-compartment electrochemical cell. The platinum disk working electrode (area 0.02 cm^2) was treated by polishing with 0.05 μm alumina on a microcloth and then sonicated for 5 min in deionized water followed by rinsing with the solvent used in the electrochemical studies. An $Ag/AgNO_3$ (0.1 M in CH_3CN) electrode was used as reference electrode. The potential of the $Ag/AgNO_3$ reference electrode was calibrated against the ferrocenium/ferrocene couple before and after each set of experiments to ensure the accuracy of the potential measured;[61a] the $E_{1/2}$ of $Cp_2Fe^{+/0}$ was found to be 0.06 ± 0.01 V vs the $Ag/AgNO_3$ reference. The $E_{1/2}$ values are the average of the cathodic and anodic peak potentials for the oxidative and reductive waves of reversible couples.[61b]

Synthesis of $[Pt_2(dppm)_2(\mu\text{-}\eta^1\text{:}\eta^1\text{-HC=CFc})Cl_2]$ (1). A methanol suspension of $[Pt_2(dppm)_2Cl_2]$ (1.0 g, 0.8 mmol) and ethynylferrocene (0.17 g, 0.8 mmol) was stirred at room temperature for 12 h, and the orange precipitate formed was filtered. The solid was dissolved in dichloromethane and filtered. Excess diethyl ether was added to the filtrate to precipitate the product as an orange solid. The product was purified by diffusing diethyl ether into a dichloromethane solution. Yield: 45%. Anal. Calcd for $C_{62}H_{54}Cl_2FeP_4Pt_2$: C, 51.7; H, 3.8. Found: C, 50.9; H, 3.8. ^1H NMR (300 MHz, $CDCl_3$, δ/ppm): 2.32 (s, 1H, H−C=); 3.26 (m, 2H, PCH_2P); 3.38 (s, 5H, C_5H_5); 3.43 (s, 2H, H2 and H5 of C_5H_4); 3.50 (s, 2H, H3 and H4 of C_5H_4); 3.77 (m, 2H, PCH_2P); 6.5−7.9 (m, 40H, Ph). $^{31}P\{^1H\}$ NMR (300 MHz, $CDCl_3$, δ/ppm): 3.14 (m, 2P, $^1J_{Pt-P}$ = 8676, $^2J_{Pt-P}$ = 342, $^1J_{P-P}$ = 57 $^2J_{P-P}$ = 27 Hz), 5.40 (m, 2P, $^1J_{Pt-P}$ = 8532, $^2J_{Pt-P}$ = 282, $^1J_{P-P}$ = 57, $^2J_{P-P}$ = 27 Hz).

Synthesis of $[Ag_3(dppm)_3(\mu_3\text{-}\eta^1\text{-C}{\equiv}\text{CFc})]\cdot 2CF_3SO_3$ ($2\cdot 2CF_3SO_3$). To a CH_2Cl_2/CH_3OH (1:1) solution (30 mL) of silver triflate (0.5 g, 1.9 mmol) were added ethynylferrocene (0.13 g, 0.6 mmol) and excess KOH (∼0.1 g), and the mixture was stirred for 24 h. The resulting orange solution was filtered, and its volume was reduced to ∼10 mL by rotaevaporation. Addition of excess diethyl ether to the solution precipitated the product. Slow diffusion of diethyl ether into an acetonitrile solution of the compounds gave orange crystals. Yield: 60%. Anal. Calcd for $C_{89}H_{75}Ag_3F_6FeO_6P_6S_2$: C, 53. 9; H, 3.8. Found: C, 53.1; H, 3.3. ^1H NMR (300 MHz, $CDCl_3$): δ 3.63 (m, 6H, PCH_2P); 4.16, 4.42 (m, 9H, Cp); 7.02−7.25 (m, 60H, Ph). $^{31}P\{^1H\}$ NMR (300 MHz, $CDCl_3$): δ 4.19, $^1J_{Ag-P}$ = 960 Hz. IR (KBr): 2013 cm^{-1}, weak, ν(C≡C).

Synthesis of $[Cu_3(dppm)_3(\mu_3\text{-}\eta^1\text{-C}{\equiv}\text{CFc})_2]PF_6$ ($3\cdot PF_6$). To a CH_2Cl_2/CH_3OH (1:1) solution (30 mL) of $[Cu_2(dppm)_2(CH_3CN)_2]\cdot 2PF_6$ (1.0 g, 0.8 mmol) were added ethynylferrocene (0.23 g, 1.1 mmol) and excess KOH (∼0.2 g), and the mixture was stirred for 24 h. The resulting orange solution was filtered, and its volume was reduced to ∼10 mL. Addition of excess diethyl ether to the solution precipitated an orange solid. Slow diffusion of diethyl ether into an acetonitrile solution of the compounds gave orange crystals. Yield: 75%. Anal. Calcd for $C_{99}H_{84}Cu_3F_6Fe_2P_7$: C, 62.3; H, 4.4. Found: C, 60.9; H, 4.4. ^1H NMR (300 MHz, $CDCl_3$): δ 6.8−7.2 (m, 60H, Ph), 4.40−4.50 (m, 18H, Cp), 3.15 (b, 6H, PCH_2P). $^{31}P\{^1H\}$ NMR (300 MHz, $CDCl_3$): δ −6.16 (s). IR (KBr): 2013 cm^{-1} (w); ν(C≡C).

In Situ Preparation of $[Cu_3(dppm)_3(\mu_3\text{-}\eta^1\text{-C}{\equiv}\text{CFc})_2]\cdot 2PF_6$ ($3\cdot 2PF_6$). To an acetonitrile solution of $3\cdot PF_6$ (4 mL, 3.1×10^{-3} M) in 1 cm UV cell was added 1 equiv of Cp_2FePF_6 (4.4 mg, 0.13 mmol), and the mixture was stirred for 10 min, during which its color changed from orange to deep red. The solution was immediately used for NIR absorption measurement.

X-ray Crystallography. The diffraction experiments were carried out on a Bruker AXS SMART CCD 3-circle diffractometer with a sealed tube at 23 °C using graphite-monochromated Mo Kα radiation (λ = 0.71073 Å). The software used were SMART[62] for collecting frames of data, indexing reflection, and determination of lattice parameters; SAINT[62] for integration of intensity of reflections and scaling; SADABS[63] for empirical absorption correction; and SHELXTL[64] for space group determination, structure solution, and least-squares refinements on $|F|^2$. The crystals were mounted at the end of glass fibers and used for the diffraction experiments. Anisotropic thermal parameters were refined for the rest of the non-hydrogen atoms. The hydrogen atoms were placed in their ideal positions. A brief summary of crystal data and experimental details is given in Table 1.

$[Pt_2(dppm)_2(\mu\text{-}\eta^1\text{:}\eta^1\text{-HC=CFc})Cl_2]\cdot Et_2O$ ($1\cdot Et_2O$). Totally 24 293 reflections were collected in the 2θ range, 1.75−26.37° ($-17 \le h \le 16$, $-18 \le k \le 18$, $-22 \le l \le 22$), of which 12 105 (R_{int} = 0.0528) were independent reflections. The diethyl ether is disordered. An extinction coefficient was refined to 0.00038(10). The electron densities fluctuated between 2.394 and −2.908 e $Å^{-3}$ in the final Fourier difference map.

$[Ag_3(dppm)_3(\mu_3\text{-}\eta^1\text{-C}{\equiv}\text{CFc})]\cdot 2CF_3SO_3\cdot H_2O$ ($2\cdot 2CF_3SO_3\cdot H_2O$). Totally 43 813 reflections were collected in the 2θ range, 1.63−25.00° ($-18 \le h \le 18$, $-63 \le k \le 24$, $-19 \le l \le 19$), of which 15 282 (R_{int} = 0.0321) were independent reflections. The Cp ring is disordered. Two different conformations have been resolved with occupancies of 0.4 and 0.6. In addition, the CF_3SO_3 anion attached to the silver atoms was disordered. The disorder can be described in terms of a rotation of the O(1)−S(1) axis. Common isotropic thermal parameters were refined for each group. An extinction coefficient was refined to 0.00079(7). Three leftover electron density peaks in the Fourier difference map were assigned to oxygen atoms of the disordered water molecules (occupancy 0.3333 for each). The electron densities fluctuated between 1.259 and −0.682 e $Å^{-3}$ in the final Fourier difference map.

$[Cu_3(dppm)_3(\mu_3\text{-}\eta^1\text{-C}{\equiv}\text{CFc})_2]\cdot PF_6$ ($3\cdot PF_6$). Totally 44 885 reflections were collected in the 2θ range, 1.68−25.00° ($-24 \le h \le 26$, $-13 \le k \le 21$, $-41 \le l \le 38$), of which 16 083 (R_{int} = 0.0444) were independent reflections. One of the phenyl rings (C1H−C6H) has large thermal parameters, and no

(58) Rodriquez, J.-G.; Oñate, A.; Martin-Villami, R. M.; Fonseca, I. *J. Organomet. Chem*. **1996**, *513*, 71.
(59) Brown, M. P.; Puddephatt, R. J. Rashidi, M. *J. Chem. Soc., Dalton Trans*. **1977**, 951.
(60) Connelly, N. G.; Geiger, W. E. *Chem. Rev*. **1996**, *96*, 877.
(61) (a) Gritzner, G.; Kùta, J. *Pure Appl. Chem*. **1982**, *54*, 1527 (b) Gagné, R. R.; Koval, C. A. Lisensky, G. C. *Inorg. Chem*. **1980**, *19*, 2855.
(62) *SMART & SAINT Software Reference Manuals*, Version 4.0; Siemens Energy & Automation, Inc., Analytical Instrumentation: Madison, WI, 1996.
(63) Sheldrick, G. M. *SADABS*, a software for empirical absorption correction; University of Gottingen: Gottingen, Germany, 1996.
(64) *SHELXTL Reference Manual*, Version 5.03; Siemens Energy & Automation, Inc., Analytical Instrumentation: Madison, WI, 1996.

Table 1. Crystal Data and Structure Refinement Details for $1\cdot Et_2O$, $2\cdot 2CF_3SO_3\cdot H_2O$, and $3\cdot PF_6$

	$1\cdot Et_2O$	$2\cdot 2CF_3SO_3\cdot H_2O$	$3\cdot PF_6$
formula	$C_{66}H_{64}Cl_2FeOP_4Pt_2$	$C_{89}H_{77}Ag_3F_6FeO_7P_6S_2$	$C_{99}H_{84}Cu_3F_6Fe_2P_7$
cryst size (mm)	0.4 × 0.2 × 0.14	0.40 × 0.38 × 0.16	0.30 × 0.22 × 0.08
cryst syst	triclinic	monoclinic	monoclinic
space group	$P\bar{1}$	$P2(1)/c$	$P2(1)/c$
lattice params (Å)	a = 13.6887(1), b = 14.4719(2), c = 17.7935(2)	a = 14.1959(1), b = 47.4768(3), c = 14.4358(2)	a = 20.1214(3), b = 15.6884(2), c = 30.8735(3)
	α = 81.340(1)°; β = 76.153(1)°; γ = 63.728(1)°	α = 90°; β = 116.12(1)°; γ = 90°	α = 90°; β = 108.216(1)°; γ = 90°
V (Å^3)	3064.91(6)	8735.53(15)	9257.5(2)
Z	2	4	4
density(calc) (g/cm^3)	1.641	1.521	1.368
abs coeff (mm^{-1})	5.019	1.049	1.162
F(000)	1488	4036	3904
no. of params varied	672	1004	987
final R indices[a]	R1 = 0.0628, wR2 = 0.1541	R1 = 0.0571, wR2 = 0.1298	R1 = 0.0627, wR2 = 0.1619
goodness of fit (GOF)[b]	1.164	1.155	1.036

[a] $R1 = (||F_o| - |F_c||)/(|F_o|)$; $wR2 = [w(F_o^2 - F_c^2)/w(F_o^4)]^{1/2}$. [b] $GOF = [(w(F_o^2 - F_c^2)^2/(n - p)]^{1/2}$. For all crystal determinations, scan type and wavelength of radiation used is ω and 0.71073 Å, respectively.

satisfactory disorder model could be found. As a result, the carbon atoms in the ring were treated as a regular hexagon. The fluorine atoms of the PF_6 anion were disordered. Two orientations of fluorine atoms were included in the model with occupancies of 0.6 and 0.4. Common isotropic thermal parameters were refined for each group. An extinction coefficient was refined to 0.00038(10). The electron densities fluctuated between 1.022 and −0.708 e Å^{-3} in the final Fourier difference map.

Results and Discussion

Syntheses and Structures. Binuclear complex $[Pt^I_2(dppm)_2Cl_2]$ is known to react with a variety of unsaturated compounds X such as CO, nitriles, and acetylenes to form the so-called A-frames $Pt_2(\mu\text{-X})$.[65−68] This addition reaction was used in this study to anchor a redox-active ferrocenyl (Fc) group on a binuclear Pt complex. Our study shows that ethynylferrocene reacts readily with $[Pt^I_2(dppm)_2Cl_2]$ to give the complex $[Pt_2(dppm)_2(\mu\text{-}\eta^1\text{:}\eta^1\text{-HC=CFc})Cl_2]$ (**1**). Single-crystal X-ray diffraction shows that **1** is composed of a bimetallic core wherein the two tetracoordinate Pt centers are bridged by two *trans*-oriented dppm and one ethynylferrocene (Figure 1a and Table 2). The fourth ligand of the metal is a chloride. Like many Pt^{II} complexes, the Pt(1) center shows a square-planar geometry. On the other hand, the Pt(2) shows some distortion, with a bent P(3)−Pt(2)−P(4) linkage of 159.64(9)°. Similar to many other dppm-bridged binuclear compounds, the orientation of the two methylene groups gives the $Pt_2(P-C-P)_2$ metallacycle a boat conformation. The long Pt−Pt separation of 3.2367(5) Å precludes any formal bonding between the metal ions, consistent with the idea that the reaction between $Pt_2(dppm)_2Cl_2$ and ethynylferrocene is an oxidative addition in which the two d^9 Pt^I ions are formally oxidized to d^8 Pt^{II}. In this context, it is noted that the C−C bond in the bridging acetylene shows a distance of 1.293(1) Å, closer to a C=C double bond (1.34 Å) than to a C≡C triple bond (1.20 Å).[69] In addition, the Pt(1)−C(11)−C(12) and Pt(1)−C(11)−C(1) angles are close to 120°, the ideal bond angle of an sp^2 carbon. Given all these structural features, it is apt to consider **1** as a diplatinated alkene in which two Pt^{II} ions are bridged by a dianionic ethylene [H−C=C−Fc]$^{2-}$. It is noted that no ν(C≡C) vibration is observed in the IR spectrum of **1**. The $^{31}P\{^1H\}$ NMR spectrum of the complex shows two signals flanked with ^{195}Pt satellites at δ 3.14 and 5.40, in accord with the X-ray crystal structure of the complex.

Reacting $Ag_2(dppm)_2(CF_3SO_3)_2$ with ferrocenylacetylide gives rise to the monoacetylide $[Ag^I_3(dppm)_3(\mu_3\text{-}\eta^1\text{-C=CFc})]\cdot 2CF_3SO_3$ (**2**$\cdot 2CF_3SO_3$). However, the diacetylide $[Ag_3(dppm)_3(\mu_3\text{-}\eta^1\text{-C≡CFc})_2]^+$ remains elusive even when a large excess of ferrocenylacetylide was used in the same reaction. The X-ray crystal structure and selected structural parameters of the complex are depicted in Figure 1b and Table 3, respectively. The main structural feature of the complex is a trinculear silver core capped by one FcC≡C$^-$ and bridged by three dppm. The silver atoms show a compressed trigonal pyramidal coordination geometry, and the average P−Ag−P and P−Ag−C angles are 124.48(5)° and 115.27(1)°, respectively. The capping of FcC≡C$^-$ is slightly asymmetric, as the Ag−C distances range from 2.245(5) to 2.320(6) Å. Similar Ag−C distances and distortions are found in the analogous complex $[Ag_3(dppm)_3(C\equiv C-C_6H_4\text{-}NO_2\text{-}p)]^{2+}$ (d(Ag−C) = 2.224(5)−2.349(6) Å).[70] The average capping angle, defined as Ag−C(1)−Ag, is 90.7(2)°. The three Ag−Ag distances are very close (average dAg−Ag = 3.2465(6) Å), and they are in the range of Ag−Ag distances observed in clusters such as $[Ag_3(dppm)_3(\mu_3\text{-}\eta^1\text{-C≡CPh})_2]^+$ (2.866(2)−2.9983(1) Å)[71] and $[Ag_3(dppm)_3(\mu_3\text{-}\eta^1\text{-C≡C}-C_6H_4\text{-}NO_2\text{-}p)]^{2+}$ (2.9850(6)−3.4030(6) Å).[70] The three Ag−Ag vectors are shorter than the sum of van der Waals radii of two Ag atoms (~3.4 Å), suggesting that metal−metal interaction is possible. One of the CF_3SO_3 anions is disordered and associated with the trinuclear silver core. The interaction between the ions is believed to be mainly electrostatic in nature, as the Ag−O distances (2.743(6)−3.280(8) Å) are longer than a normal Ag−O covalent bond (~2.3−2.6 Å). The X-ray structure of the

(65) Grossel, M. C.; Moulding, R. P.; Seddon, K. R. *Inorg. Chim. Acta* **1983**, *64*, L275.
(66) Brown, M. P.; Puddephatt, R. J.; Rashidi, M.; Seddon, K. R. *J. Chem. Soc., Dalton Trans.* **1978**, 1540.
(67) Grundy, K. R.; Robertson, K. N. *Organometallics* **1983**, *2*, 1736.
(68) Balch, A. L.; Benner, L. S.; Olmstead, M. M. *Inorg. Chem.* **1979**, *18*, 2996.
(69) Eliel, E. L.; Wilen, S. H. *Stereochemistry of Organic Compounds*; Wiley-Interscience: New York, 1994; p 13.
(70) Yam, V. W. W.; Fung, W. K. M.; Cheung, K. K. *Organometallics* **1997**, *16*, 2032.
(71) Wang, C. M.; Peng, S. M.; Chan, C. K.; Che, C. M. *Polyhedron* **1996**, *15*, 1853.

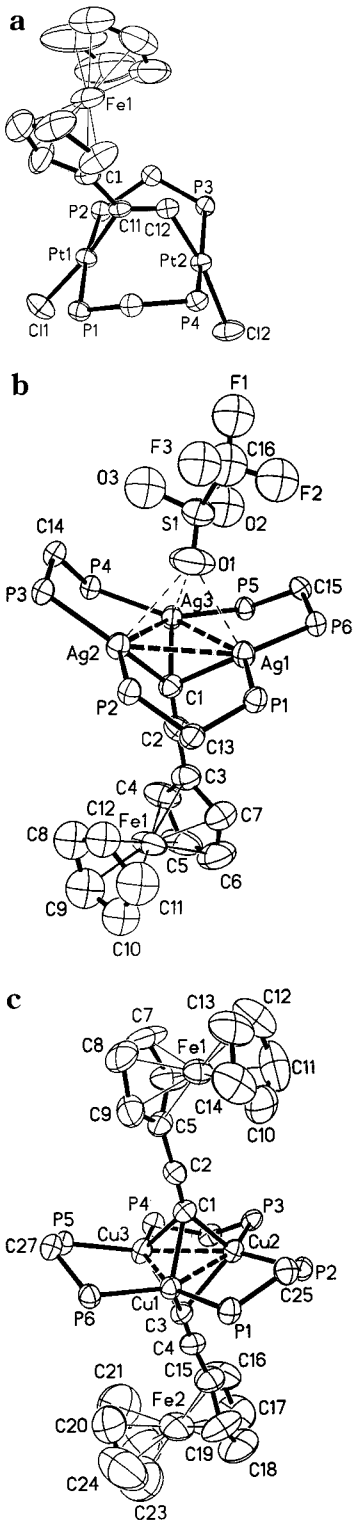

Figure 1. ORTEP plots (thermal ellipsoid = 50%) of (a) **1**·Et_2O, (b) **2**·$2CF_3SO_3$·H_2O, and (c) **3**·PF_6. All phenyl rings and hydrogen atoms are removed. All the anions are not shown except the one associated with the silver atoms in $\mathbf{2}^{2+}$.

Ag complex deviates slightly from the ideal C_{3v} symmetry; that is, the three Ag−C bonds (or Ag−Ag vectors) have slightly different lengths. Nevertheless the complex reverts to C_{3v} symmetry in solution, as the $^{31}P\{^1H\}$ NMR spectrum of the compound at room temperature shows only a sharp doublet at 4.19 ppm with a $^1J_{Ag-P}$ of 960 Hz.

Table 2. Selected Bond Lengths (Å) and Angles (deg) for 1·Et_2O

Pt(1)−Pt(2)	3.32367(5)	P(1)−Pt(1)−P(2)	173.59(9)
Pt(1)−C(11)	2.030(9)	P(3)−Pt(2)−P(4)	159.64(9)
Pt(2)−C(12)	2.021(9)	Pt(1)−C(11)−C(12)	120.4(7)
Pt(1)−P(1)	2.274(2)	Pt(1)−C(11)−C(1)	116.7(7)
Pt(1)−P(2)	2.272(2)	Pt(2)−C(12)−C(11)	116.8(7)
Pt(2)−P(3)	2.294(2)	C(1)−C(11)−C(12)	122.6(8)
Pt(2)−P(4)	2.300(2)	Cl(1)−Pt(1)−C(11)	172.8(3)
C(11)−C(12)	1.293(1)	Cl(1)−Pt(1)−P(1)	94.28(9)
Pt(1)−Cl(1)	2.397(3)	Cl(2)−Pt(2)−C(12)	171.0(3)
		Cl(2)−Pt(2)−P(3)	103.02(1)

Table 3. Selected Bond Lengths (Å) and Angles (deg) for 2·$2CF_3SO_3$·H_2O

Ag(1)−Ag(2)	3.2451(6)	Ag(1)−Ag(2)−Ag(3)	59.851(1)
Ag(1)−Ag(3)	3.2416(6)	Ag(2)−Ag(1)−Ag(3)	60.191(1)
Ag(2)−Ag(3)	3.2527(6)	Ag(1)−Ag(3)−Ag(2)	59.958(1)
Ag(1)−P(1)	2.4740(1)	Ag(1)−C(1)−Ag(2)	90.6(2)
Ag(1)−P(6)	2.4551(1)	Ag(1)−C(1)−Ag(3)	89.6(2)
Ag(2)−P(3)	2.4804(2)	Ag(2)−C(1)−Ag(3)	91.9(2)
Ag(1)−C(1)	2.320(6)	C(1)−Ag(1)−Ag(2)	43.78(1)
Ag(2)−C(1)	2.245(5)	C(1)−Ag(1)−P(1)	108.82(1)
Ag(3)−C(1)	2.281(6)	C(1)−Ag(1)−P(6)	120.95(1)
C(1)−C(2)	1.206(8)	P(1)−Ag(1)−P(6)	123.06(5)
Ag(1)−O(1)	2.743(6)		
Ag(2)−O(1)	2.817(6)		
Ag(3)−O(1)	3.280(8)		

Table 4. Selected Bond Lengths (Å) and Angles (deg) for 3·PF_6

Cu(1)−Cu(2)	2.6006(9)	Cu(1)−Cu(2)−Cu(3)	59.00(2)
Cu(1)−Cu(3)	2.5970(9)	Cu(2)−Cu(1)−Cu(3)	61.88(2)
Cu(2)−Cu(3)	2.6722(9)	Cu(1)−Cu(3)−Cu(2)	59.13(2)
Cu(1)−P(1)	2.291(2)	Cu(1)−C(1)−Cu(2)	74.8(2)
Cu(2)−P(3)	2.2861(2)	Cu(1)−C(1)−Cu(3)	69.1(2)
Cu(3)−P(5)	2.2828(2)	Cu(2)−C(1)−Cu(3)	72.9(2)
Cu(1)−C(1)	2.184(5)	Cu(1)−C(3)−Cu(2)	70.8(2)
Cu(2)−C(1)	2.094(5)	Cu(1)−C(3)−Cu(3)	74.4(2)
Cu(3)−C(1)	2.386(5)	Cu(2)−C(3)−Cu(3)	73.8(2)
Cu(1)−C(3)	2.168(6)	C(1)−Cu(1)−Cu(2)	51.00(1)
Cu(2)−C(3)	2.316(6)	C(3)−Cu(1)−Cu(2)	57.26(2)
Cu(3)−C(3)	2.128(6)	C(1)−Cu(2)−Cu(3)	58.59(2)
C(1)−C(2)	1.201(7	C(1)−Cu(1)−Cu(3)	59.12(1)
		P(1)−Cu(1)−P(6)	111.30(6)
		C(1)−Cu(1)−P(1)	106.21(2)
		C(1)−Cu(1)−P(6)	108.95(2)
		C(3)−Cu(1)−P(1)	116.5(2)
		C(3)−Cu(1)−P(6)	116.1(2)
		C(1)−Cu(1)−C(3)	95.9(2)
		C(1)−Cu(2)−C(3)	95.9(2)
		C(1)−Cu(3)−C(3)	95.9(2)

The diacetylide $[Cu^I_3(dppm)_3(\mu_3\text{-}\eta^1\text{-}C{\equiv}CFc)_2]$·$PF_6$ (**3**·PF_6) was prepared by reacting $Cu^I_2(dppm)_2(CH_3CN)_2$·$2PF_6$ with 4/3 equiv of ethynylferrocene in the presence of excess potassium hydroxide.[53] The X-ray crystal structure and selected structural parameters of the cation $\mathbf{3}^+$ are displayed in Figure 1c and Table 4, respectively. The cation $\mathbf{3}^+$ is composed of a triangular copper core in which the metal atoms are bridged by three dppm ligands and capped by two $FcC{\equiv}C^-$. The Cu^I ions show a distorted tetrahedral coordination geometry; for instance, the P−Cu(1)−P and P−Cu(1)−C angles are close to the ideal 109°, while the C(1)−Cu(1)−C(3) angle is only 95.9(2)° (Table 5). The average capping angles, defined as Cu−C(1/3)−Cu, are 72.3(2)° and 73.0(2)°. It is noted that the three Cu−Cu distances are close (average 2.6233(2) Å) and similar to the ones in the analogous complex $[Cu_3(dppm)_3(\mu_3\text{-}\eta^1\text{-}C{\equiv}CPh)_2]^+$ (dCu−Cu = 2.570(3)−2.615(3) Å).[53] The two Fc groups show an *anti*-conformation in the solid state, and the separation of the two iron atoms is 11.777(6) Å. The

Table 5. Reduction Potentials and K_c of Compounds 1, 2·2CF$_3$SO$_3$, and 3·PF$_6$ in Comparison with Other Bis(ferrocenylacetylide) Compounds

D−M−A[a]	$E_{1/2}$ (1st Fc oxidation)[b]/mV	$E_{1/2}$ (2nd Fc oxidation)/mV	ΔE_p/mV	$\Delta E_{1/2}$/mV	K_c	ref
1	−48 ± 10		60			this work
2·2CF$_3$SO$_3$	235 ± 10		140			this work
3·PF$_6$	114 ± 10	224 ± 10	60	110 ± 10	77 ± 30	this work
trans-{[Pt[P(*p*-tosyl)$_3$]$_2$(C≡CFc)$_2$	63	143	100	80	23	36
trans-[Pt(PMePh$_2$)$_2$(C≡CFc)$_2$]	83	163	100	80	23	36
trans-[Ru(PBu$_3$)$_2$(CO)$_2$(C≡CFc)$_2$]	−47 ± 10	43 ± 10		90 ± 10	35	33
trans-[Ru(dppm)$_2$(C≡CFc)$_2$]	−297 ± 10	−77 ± 10	70	220 ± 10	6100 ± 2500	32−34
trans-[Ru(dppe)$_2$(C≡CFc)$_2$]	−330	−45		285	1.2×10^5	39

[a] Solvents used for voltammetric measurements: CH$_3$CN (0.1 M *n*-Bu$_4$NClO$_4$) for **2**·2CF$_3$SO$_3$ and **3**·PF$_6$; for the rest CH$_2$Cl$_2$ (with 0.1 M *n*-Bu$_4$NPF$_6$). [b] vs Ag/AgNO$_3$ (0.1 M).

X-ray crystal structure of **3**$^+$ shows that the geometry deviates from maximum D_{3h} symmetry, as the capping of the FcC≡C$^-$ is not symmetric. The acetylides are slanted toward two of the copper atoms: Cu(1)−C(1) (2.184(5) Å) and Cu(2)−C(1) (2.094(5) Å) bonds are shorter than the Cu(3)−C(1) (2.386(5) Å) bond and the other capping atom C(3) is closer to Cu(1) (Cu(1)−C(3), 2.168(6) Å) and Cu(2) (Cu(3)−C(3), 2.128(6) Å) than Cu(2) (Cu(2)−Cu(3), 2.316(6) Å). Similar distortion has been observed in [Cu$_3$(dppm)$_3$(μ_3-η^1-C≡CPh)$_2$]$^+$.[53] Nonetheless, the solution ^{31}P{^{1}H} NMR spectrum of the complex exhibits only a sharp singlet at −6.16 ppm, indicating that all three dppm and hence copper atoms are equivalent. Apparently the coordination core of **3**$^+$ restores to a local D_{3h} symmetry in solution, as the two FcC≡C$^-$ adopt a centrosymmetric capping position. The two Fc groups are equivalent, as only one set of Fc signals is discerned in the ^{1}H NMR spectrum.

Spectroscopic and Electrochemical Properties. The solution UV−vis absorption spectrum of **1** displays a weak band at 485 nm (ϵ_{max} = 775 M^{-1} cm^{-1}) assignable to the ligand field transition of the Fc group. Analogous absorption bands are found in the spectra of **2**·2CF$_3$SO$_3$ (λ_{max} = 448 nm, ϵ_{max} = 510 M^{-1} cm^{-1}) and **3**·PF$_6$ (λ_{max} = 458 nm; ϵ_{max} = 1560 M^{-1} cm^{-1}) as well. In addition to the ligand field absorption band, the spectrum of **3**·PF$_6$ shows a shoulder around 350 nm (ϵ = 4400 M^{-1} cm^{-1}) which is also observed in the spectra of related complexes such as [Cu$_3$(dppm)$_3$(μ_3-η^1-C≡CPh)$_2$]$^+$ [54] and [Cu$_3$(PNP)$_3$(μ_3-η^1-C≡CX)$_2$]$^+$ (X = 4-substituted phenyl, PNP = PPh$_2$NRPPh$_2$, R = alkyl/aryl).[55] On the basis of previous studies, the absorption shoulder is attributed to a metal-perturbed $\pi\rightarrow\pi^*$ or Cu$_3\rightarrow\pi^*$(FcC≡C) MLCT transition.

The electronic properties of the three ferrocenyl-bearing complexes were gauged by voltammetric techniques. Room-temperature cyclic voltammogram (CV) of **1** shows a reversible oxidation (ΔE_p = 60 mV, i_c/i_a = 1) at −48 ± 10 mV vs Ag/AgNO$_3$ (Figure 2a) attributable to the one-electron oxidation of the Fc group. In addition, there is an irreversible oxidation at 643 ± 10 mV which likely corresponds to the oxidation of the Pt, the only redox-active center in the complex other than the Fc group. Corresponding Pt reduction occurs at 403 ± 10 mV. No reduction wave appears in the cathodic sweep. The room-temperature CV of **2**·2CF$_3$SO$_3$ is shown in Figure 2b. The compound exhibits a quasi-reversible oxidation at 235 ± 10 mV vs Ag/AgNO$_3$ (ΔE_p= 140 ± 10 mV, $i_c/i_a \approx 1$) in the anodic sweep which is assigned to the one-electron oxidation of the Fc group, as no such an oxidation wave is observed in the CV of [Ag$_3$(dppm)$_3$(μ_3-η^1-C≡C-C$_6$H$_4$-NO$_2$-*p*)]$^{2+}$.[70] An irreversible oxidation appears at ∼1.1 V which is probably due to an oxidation at the silver cluster. Figure 2c shows the CV of **3**·PF$_6$ measured in acetonitrile at 298 K. In the anodic sweep, two reversible oxidation waves ($\Delta E_p \approx$ 60 mV, $i_c/i_a \approx 1$) of similar area occur at ∼150 mV vs Ag/AgNO$_3$. The waves are duly assigned to the successive oxidations of the two Fc groups of **3**$^+$, as no such oxidation is found in the CV of [Cu$_3$(dppm)$_3$(μ-η^1-C≡CPh)$_2$]$^+$.[54]

$$[Fc^{II}Cu_3Fc^{III}]^{2+} + e^- \rightleftharpoons [Fc^{II}Cu_3Fc^{II}]^{+} \quad E_{1/2} = 114 \pm 10\text{mV} \text{ vs Ag/AgNO}_3$$
$$\mathbf{3^{2+}} \qquad\qquad \mathbf{3^{+}}$$

$$[Fc^{III}Cu_3Fc^{III}]^{3+} + e^- \rightleftharpoons [Fc^{II}Cu_3Fc^{III}]^{+} \quad E_{1/2} = 224 \pm 10\text{ mV}$$
$$\mathbf{3^{3+}} \qquad\qquad \mathbf{3^{2+}}$$

The oxidations are better resolved in the differential pulse voltammogram (Figure 2d), wherein two peaks with almost equal intensity appear at 114 ± 10 and 224 ± 10 mV (vs Ag/AgNO$_3$; scan rate = 20 mV/s; pulse width = 50 ms). On the basis of the potential difference ($\Delta E_{1/2}$) of the two Fc oxidations (110 ± 14 mV), the comproportionation constant for reaction 1 (K_c) is found to be 77 ± 30 (eq 1).

$$[Fc^{II}Cu_3Fc^{II}]^{+} + [Fc^{III}Cu_3Fc^{III}]^{3+} \rightleftharpoons 2[Fc^{II}Cu_3Fc^{III}]^{2+} \quad K_c \text{ (reaction 1)}$$
$$\mathbf{3^{+}} \qquad\qquad \mathbf{3^{3+}} \qquad\qquad \mathbf{3^{2+}}$$

$$\ln K_c = \frac{F}{RT}\Delta E_{1/2} \qquad (1)$$

In addition to the Fc oxidations, the CV of **3**·PF$_6$ also shows irreversible oxidation and reduction peaks at 1046 ± 10 and 509 ± 10 mV, respectively ($i_c/i_a \sim$ 0.06). On the basis of the results of previous studies, the peaks are assigned to oxidation and reduction at the tricopper core. Most of the [Cu$_3$(P∧P)$_3$(μ_3-η^1-C≡CR)$_2$]$^+$ complexes exhibit quasi-reversible oxidation at the tricopper core. However the copper oxidation in [Cu$_3$(dppm)$_3$(μ_3-η^1-C≡C−C$_6$H$_4$-NO$_2$-*p*)$_2$]$^+$ is irreversible, as the electron-deficient 4-nitrophenylacetylide ligands fail to stabilize the Cu^{II} ion formed in the oxidation.[56] The irreversible oxidation in the CV of **3**·PF$_6$ appears after the two Fc oxidations; possibly the oxidized ferrocenylacetylides, being less electron-donating, are unable to stabilize the Cu^{II} ion arising from oxidation. Unlike analogous compounds such as [Ag$_3$(dppm)$_3$(μ_3-η^1-C≡C-C$_6$H$_4$-NO$_2$-*p*)]$^{2+}$ [70] and [Cu$_3$(dppm)$_3$(μ_3-η^1-C≡C-C$_6$H$_4$-NO$_2$-*p*)$_2$]$^+$,[56] which display quasi-reversible acetylide-centered reduction, no distinct reduction wave is observed in the CVs of **2**$^{2+}$

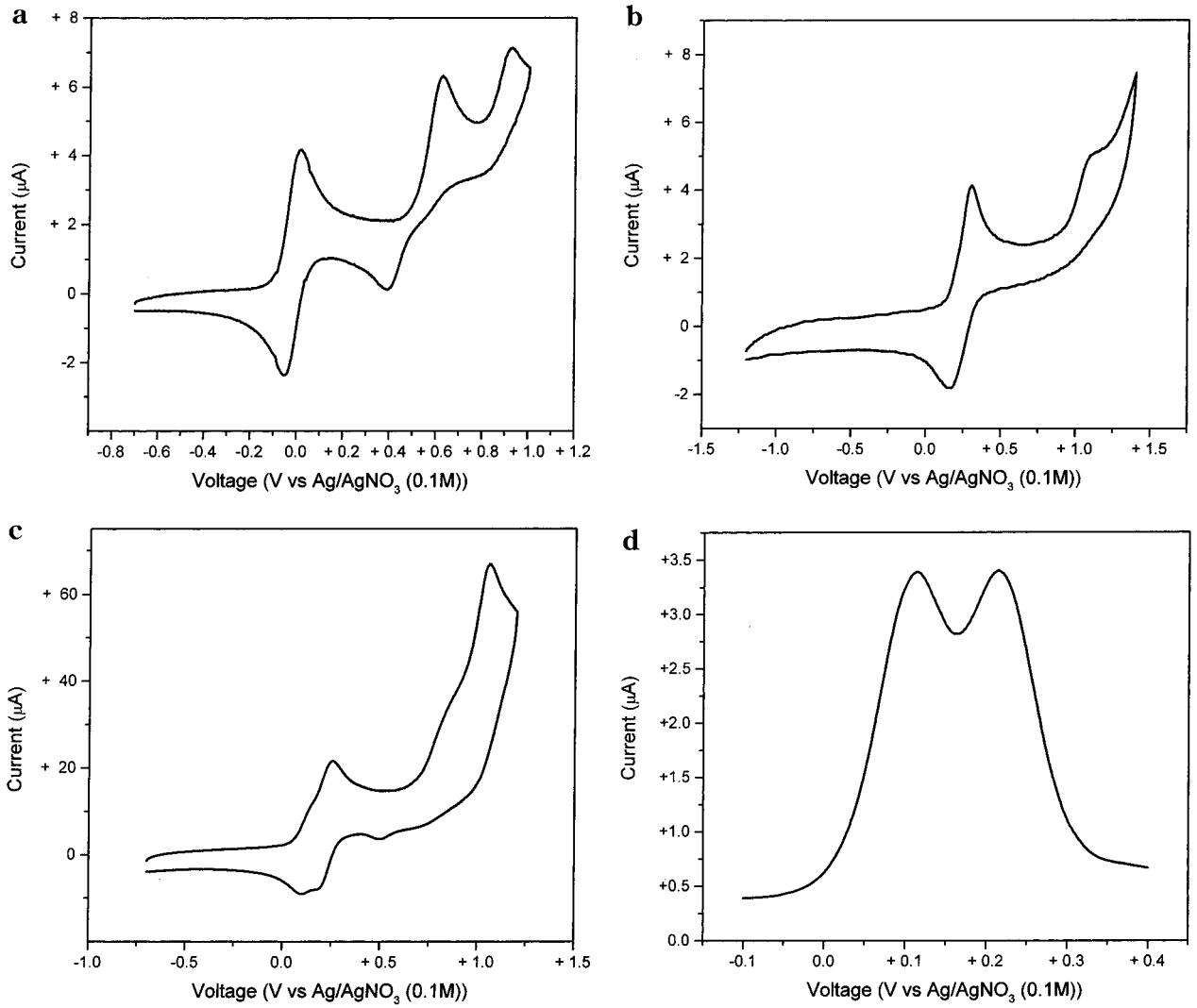

Figure 2. (a) Cyclic voltammogram of **1** in CH_2Cl_2 at room temperature; reference electrode $Ag/AgNO_3$; working electrode Pt; scan rate = 20 mV/s. (b) Cyclic voltammogram of **2**·$2CF_3SO_3$ in CH_3CN at room temperature; reference electrode $Ag/AgNO_3$; working electrode Pt; scan rate = 50 mV/s. (c) Cyclic voltammogram of **3**·PF_6 in CH_3CN at room temperature; reference electrode $Ag/AgNO_3$; working electrode Pt; scan rate = 50 mV/s. (d) Differential pulse voltammogram of **3**·PF_6 in CH_3CN at room temperature; reference electrode $Ag/AgNO_3$; working electrode Pt; scan rate = 20 mV/s, sample width = 17 ms, pulse amplitude = 50 mV, pulse width = 50 ms, pulse period = 200 ms, quiet time = 5 s.

and $\mathbf{3}^+$. Most likely the ligand-centered reduction of the complexes is beyond the widow of the solvent used.

The reduction potential of the Fc groups in the compounds follows the order $\mathbf{2}^{2+} > \mathbf{3}^+$ (1st oxidation) $\gg$ **1** (Table 5). Notably the reduction potential of **1** is exceptionally low in comparison with the free ethynylferrocene ($E_{1/2}$(FcC≡CH$^+$/FcC≡CH) = 224 mV vs $Ag/AgNO_3$).[72] This could be due to substantial charge transfer from the metal centers onto the ethynylferrocene, rendering the Fc group more electropositive. In fact EHMO calculations have shown that for the analogous A-frame complex [Pd_2(dppm)$_2$(μ-η^1:η^1-HC═CH)Cl_2] there are two electrons, transferred from the metal ions, residing in the π*-orbital of the bridging acetylene.[73] For compound **1**, the π*-orbital of the C═C bond is conjugated with the π-orbitals of the Cp ring, and the increase of electron density in the π*-orbital would lead to a more reducing Fc group, as observed. It is noted that the Fc protons of **1** (δ 3.43−3.77) are upfield shifted from those of **2**·$2CF_3SO_3$ (δ 4.16−4.42) and **3**·PF_6 (δ 4.40−4.50). This is in accord with the result of the voltammetric study that shows that the Fc group in the binuclear Pt complex is more electron rich.

Recent studies of Plenio showed that the reduction potential of Fc groups in protonated ferrocenylamines[74,75] and a series of Fc-modified 1,4,8,11-tetraazacyclotetradecane [M(Fc-Cylam)]$^{2+}$ (M = Zn^{2+}, Cu^{2+}, Ni^{2+}, Cd^{2+}, Hg^{2+}, Pb^{2+})[76] is dictated by through-space electrostatic interaction between the oxidized Fc^+ and positive charge on the protonated amine or the metal ion M coordinated to the macrocycle. The cathodic shift observed in $\mathbf{2}^{2+}$ and $\mathbf{3}^+$ indeed parallels the decrease of positive charge on the metal clusters ($Ag_3^{2+} \rightarrow Cu_3^+$). The reduction potential of Fc groups in $\mathbf{2}^{2+}$ (232 ± 10 mV) and $\mathbf{3}^+$ (1st oxidation: 114 ± 10 mV) is different by 118 ± 14 mV. In other words, the $\mathbf{3}^{2+} + e^- \rightarrow \mathbf{3}^+$ reduction is about 10

(72) Nock, H.; Schottenberger, H. *J. Org. Chem.* **1993**, *58*, 7048.
(73) Hoffman, D. M.; Hoffmann, R. *Inorg. Chem.* **1981**, *20*, 3543.
(74) Plenio, H.; Yang, J.; Diodone, R.; Heinze, J. *Inorg. Chem.* **1994**, *33*, 4098.
(75) Plenio, H.; Diodone, R. *Inorg. Chem.* **1995**, *34*, 3964.
(76) Plenio, H.; Aberle, C.; Al Shihadeh, Y.; Lloris, J. M.; Martínez-Máñez, R.; Pardo, T.; Soto, J. *Chem. Eur. J.* **2000**, *7*, 2848.

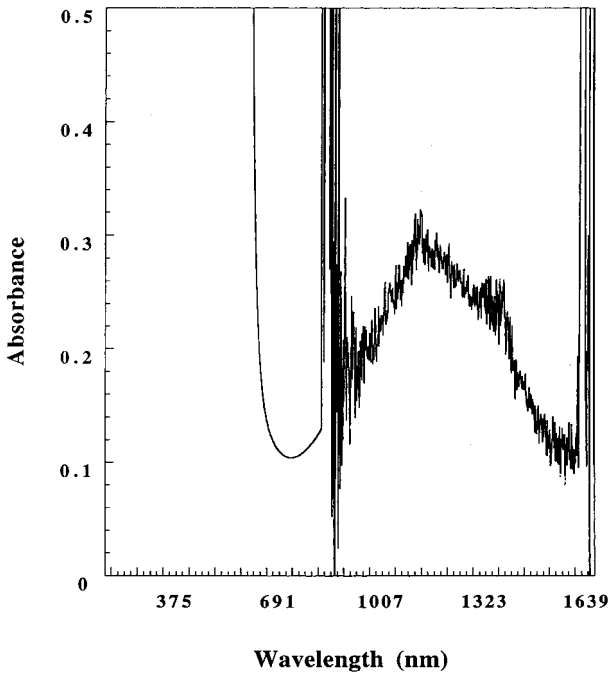

Figure 3. Near-infrared absorption spectrum of an acetonitrile solution of **3**·2PF_6 (3.14×10^{-3} M) and 1 molar equiv of Cp_2FePF_6 at room temperature. The spikes are due to solvent absorption.

kJ mol^{-1} ($\Delta G = -nF\Delta E$) less favorable than the $\mathbf{2}^{3+} + e^- \rightarrow \mathbf{2}^{2+}$ reduction. Our estimation shows that, in term of electrostatic interaction, $\mathbf{2}^{3+}$ ($\mathbf{Fc}^+\leftrightarrow\mathbf{Ag_3}^{2+}$) is less stable than $\mathbf{3}^{2+}$ ($\mathbf{Fc}^+\leftrightarrow\mathbf{Cu_3}^+$) by ~7 kJ mol^{-1}.[77] In addition, the bis(acetylide) $\mathbf{3}^+$ has one Fc group more than the monoacetylide $\mathbf{2}^{2+}$; hence statistically the oxidation of $\mathbf{2}^{2+}$ is RT ln 2 (1.7 kJ mol^{-1}) less feasible than that of $\mathbf{3}^+$. Accordingly, the $\mathbf{3}^{2+} + e^- \rightarrow \mathbf{3}^+$ reduction is about 8.7 kJ mol^{-1} less favorable than the $\mathbf{2}^{3+} + e^- \rightarrow \mathbf{2}^{2+}$ reduction. Clearly the electrostatic repulsion between the oxidized Fc^+ and the positively charged trimetallic cluster is a major factor in determining the reduction potential of $\mathbf{2}^{3+}$ and $\mathbf{3}^{2+}$.

The small K_c signifies limited electron delocalization over the cluster, and the electron is trapped in one of the Fc groups. According to the classification scheme of Robin and Day,[43] the one-electron oxidized $\mathbf{3}^{2+}$ is a class II mixed-valence complex. Attempts were made to synthesize and isolate $\mathbf{3}^{2+}$ by reacting **3**·PF_6 with oxidants such as Cp_2FePF_6 or $AgPF_6$. However no analytically pure sample of **3**·2PF_6 was obtained. This could be due to the small K_c for the formation of $\mathbf{3}^{2+}$.[78] Nonetheless, reacting **3**·PF_6 with 1 equiv of Cp_2FePF_6 gives rise to a near-infrared absorption band at ~1250 nm (Figure 3). Similar absorption bands, assigned as intervalence charge-transfer transition (IVCT), are found in the NIR spectra of class II mixed-valence complexes.[79] Thus the 1250 nm absorption is tentatively attributed to IVCT transition of the one-electron-oxidized $\mathbf{3}^{2+}$. Notably, the broad and symmetric band confirms that $\mathbf{3}^{2+}$ is a class II system as the half-height bandwidth $\Delta\nu_{1/2}$ (3800 cm^{-1}) and absorption maxima ν_{max} (8000 cm^{-1}) agree fairly well with the predicted values for class II mixed-valence complexes ($\Delta\nu_{1/2} = (2310\nu_{max})^{1/2}$ cm^{-1}).[22] Since the spectrum is very noisy, the extinction coefficient and hence electronic coupling parameter were not calculated.

The free energy change of the comproportionation (ΔG_c), a measure of the stability of the mixed-valence $\mathbf{3}^{2+}$ relative to $\mathbf{3}^+$ and $\mathbf{3}^{3+}$, is a function of electrostatic interaction (ΔG_e), statistical effect, electron delocalization over the bridge (ΔG_r), inductive effect (ΔG_i), and magnetic exchange (ΔG_{ex}) (eq 2)[80]

$$\Delta G_c = \Delta G_{c'} + \Delta G_s \qquad (2)$$

$$(\Delta G_{c'} = \Delta G_e + \Delta G_i + \Delta G_r + \Delta G_{ex})$$

The statistical factor ΔG_s amounts to $-RT$ ln 4 (−3.4 kJ mol^{-1}),[81] while the total contribution from other factors ($\Delta G_{c'}$) to the stability of $\mathbf{3}^{2+}$ (per mole) is equal to $-1/2\ RT\ \ln(K_c/4)$ or -3.7 ± 0.5 kJ mol^{-1}.[81] The electrostatic interaction, ΔG_e, is known to contribute significantly to the stability of weakly coupled class II systems. It arises from the decrease of electrostatic repulsion in the mixed-valence II,III state from the two-electron-oxidized III,III state. The parameter can be estimated using eq 3,[74−76,82] in which R_{12} stands for the distance between point charges, e the elementary charge, ϵ the relative dielectric constant of the solvent (36.7 for acetonitrile), and ϵ_o the vacuum permittivity.

$$\Delta G_e = -\frac{Ne^2}{4\pi\epsilon\epsilon_o R_{12}} \qquad (3)$$

Unlike many other D−M−A compounds that contain a neutral bridge, the bridge in the tricopper complex is cationic. The ΔG_e for the comporportionation can be estimated by calculating the intramolecular electrostatic repulsions in the three species involved in the reaction (Figure 4). As complex $\mathbf{3}^+$ bears only one positive charge, there is no intramolecular Coulombic repulsion. On the other hand, the two-electron-oxidized $\mathbf{3}^{3+}$ contains three positive charges in the two oxidized Fc^+ and the Cu_3^+ cluster, giving rise to (i) two repulsions between Fc^+ and Cu_3^+ [2($\mathbf{Fc}^+\leftrightarrow\mathbf{Cu_3}^+$)] and (ii) one between terminal Fc^+ groups ($\mathbf{Fc}^+\leftrightarrow\mathbf{Fc}^+$). The product of the reaction, $\mathbf{3}^{2+}$, carries two positive charges in Fc^+ and Cu_3^+. As the molar equivalent of $\mathbf{3}^{2+}$ is 2 times of that of $\mathbf{3}^+$ or $\mathbf{3}^{3+}$ in the reaction, there are totally two repulsions between Fc^+ and Cu_3^+ [2**($\mathbf{Fc}^+\leftrightarrow\mathbf{Cu_3}^+$)**]. Consequently, the reac-

(77) Assuming the charges of the complexes $\mathbf{2}^{3+}$ and $\mathbf{3}^{2+}$ are located in the iron atoms and the metal ions in the clusters, the difference in electrostatic repulsion between the two complexes can be estimated using eq 3 (see text), where ϵ is the dielectric constant of the solvent and R_{Fe-Ag} (5.783(6) Å) and R_{Fe-Cu} (6.079(6) Å) are the average distances between the iron and the silver and copper atoms, respectively.

$$\Delta G_e = -\frac{Ne^2}{4\pi\epsilon\epsilon_o}\left(\frac{2}{R_{Fe-Ag}} - \frac{1}{R_{Fe-Cu}}\right)$$

(78) Cotton, F. A.; Donahue, J. P.; Lin, C.; Murillo, C. A. *Inorg. Chem.* **2001**, *40*, 1234.

(79) (a) Levanda, C.; Bechgaard, K.; Cowan, D. O. *J. Org. Chem.* **1976**, *41*, 2700. (b) Ribou, A. C.; Launay, J. P.; Sachteben, M. L.; Li, H.; Spangler, C. W. *Inorg. Chem.* **1996**, *35*, 3735.

(80) Palaniappan, V.; Singru, R. M.; Agarwala, U. C. *Inorg. Chem.* **1988**, *27*, 181.

(81) (a) Sutton, J. E.; Sutton, P. M.; Taube, H. *Inorg. Chem.* **1979**, *18*, 1017. (b) Sutton, J. E.; Taube, H. *Inorg. Chem.* **1981**, *20*, 3125.

(82) (a) Ferrere, S.; Elliott, C. M. *Inorg. Chem.* **1995**, *35*, 5818. (b) Evans, C. E. B.; Naklicki, M. L.; Rezvani, A. R.; White, C. A.; Kondratiev, V. V.; Crutchley, R. J. *J. Am. Chem. Soc.* **1998**, *120*, 13096. (c) Reimers, J. R.; Hush, N. S. *Inorg. Chem.* **1990**, *29*, 3686.

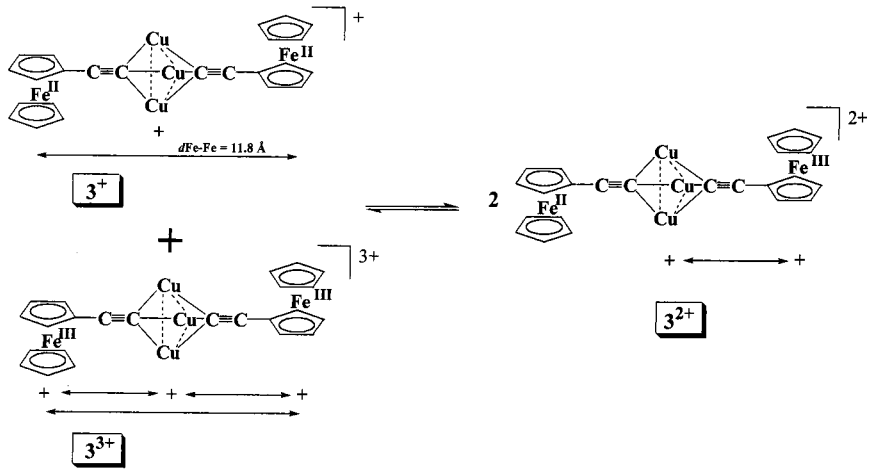

Figure 4. Diagram showing electrostatic interactions in the complexes involved in the comproportionation reaction of compound $\mathbf{3}^{2+}$.

tion leads to a net decrease of electrostatic repulsion between two Fc^+ groups ($\mathbf{Fc}^+ \leftrightarrow \mathbf{Fc}^+$). Assuming the two positive charges are localized in the iron atoms, eq 4 gives an estimated ΔG_e of -3.2 kJ mol^{-1} (R_{12} is taken as the separation between the two iron atoms (11.777(6) Å) in the X-ray crystal structure of $\mathbf{3}^+$). The value is close to $\Delta G_{c'}$ (-3.7 ± 0.5 kJ mol^{-1}), indicating that the stability of $\mathbf{3}^{2+}$ is mainly derived from the ΔG_e and ΔG_s.

$$\Delta G_e \approx -\frac{N(1.602 \times 10^{-19})^2}{4\pi\epsilon_o \times 36.7 \times 10^{-10}}\left(\frac{1}{11.8}\right) \qquad (4)$$

In other words, other factors such as ΔG_r have very marginal effect on the stability of the mixed-valence compound. The dominance of ΔG_e and ΔG_s in the stability of weakly coupled mixed-valence complexes has been previously observed in class II systems such as *E*-/*Z*-diferocenylethylene[83] and $[(NH_3)_5Ru^{II}(4,4'\text{-bipyridine})Ru^{III}(NH_3)_5]$[81] and is regarded as evidence for the inefficiency of the bridge in mediating electron delocalization.

The poor electron delocalization in $\mathbf{3}^{2+}$ could not be solely due to the long Fe−Fe separation, as compounds with similar intermetallic distance such as *trans*-$[Ru(dppm)_2(C{\equiv}CFc)_2]^+$ ($K_c = 6100 \pm 2500$)[33,34] and *trans*-$[Ru(dppe)_2(C{\equiv}CFc)_2]^+$ ($K_c = 1.2 \times 10^5$)[39] demonstrate a large degree of electron delocalization. We believed that the small extent of electron delocalization in $\mathbf{3}^{2+}$ is result of disruption of π-conjugation between the two ferrocenylacetylides. It is known that π-overlap is important to charge delocalization in mixed-valence compounds in which the metal ions are connected by a π-conjugated bridge.[4,27,32,39,84,85] Disruption of π-overlap is argued to be the reason of the poor electronic communication.[33,36,86] A telling example is the drastic difference in K_c between the compounds *trans*-$[Ru(dppm)_2(C{\equiv}CFc)_2]$ ($K_c = 61000 \pm 2500$) and *cis*-$[Ru(dppm)_2(C{\equiv}CFc)_2CuI]$ ($K_c = 260 \pm 100$).[33] The low K_c observed for *cis*-$[Ru(dppm)_2(C{\equiv}CFc)_2CuI]$ is partly due to disruption of π-overlap, as two acetylide ligands in the complex are perpendicular to each other. On the other hand, the same dπ-orbitals of Ru are involved in the back-bonding with the π^*-orbitals of the two terminal acetylide ligands in the trans-isomer, leading to a large extent of electron delocalization. The interaction between π-orbitals of acetylide and metal in $\mathbf{3}^{2+}$ can be accessed on the basis of the coordination geometry of the metal ions. Unfortunately, the X-ray crystal structure of $\mathbf{3}^{2+}$ is not available. Nevertheless, the structures of $\mathbf{3}^{2+}$ would not deviate much from that of $\mathbf{3}^+$, as redox conversion of the species is highly reversible. From the X-ray crystal structure of $\mathbf{3}^+$, it is known that the bond angles between the two acetylide and copper atoms are close to 90° (e.g., C(1)−Cu−C(3) = 95.9(2)°). If the same orthogonal arrangement of acetylide ligands and copper atoms is retained in $\mathbf{3}^{2+}$, one would expect poor overlap between the π-orbitals of the ligand and the 3d or 4p π-orbitals of the metal ions. This insufficient orbital interaction would lead to disruption of π-conjugation, hence weak electronic communication in $\mathbf{3}^{2+}$.

Conclusions

In this study we demonstrated that the redox-active ferrocenyl group could be readily attached to binuclear Pt and trinuclear Cu and Ag clusters. The low reduction potential of **1** is electrochemical evidence for a substantial electron transfer from the Pt_2 center to the bridging ethynylferrocene. On the basis of the electrochemical and structural properties, **1** is formally considered as a dimetalated alkene. Electrostatic interaction has a dominating effect on the reduction potential of the Fc groups attached to the trinuclear copper and silver clusters. Electron delocalization mediated by the C_2−Cu_3^I−C_2 linkage does not contribute significantly to the stability of the mixed-valence $\mathbf{3}^{2+}$. Conversely, the stability arises mainly from the decrease of intramolecular electrostatic repulsion and statistical distribution. The importance of the statistical distribution is shown by the fact that it contributes ~50% to the overall

(83) Chen, Y. J.; Pan, D.-S.; Chiu, C.-F.; Su, J.-X.; Lin, S. J.; Kwan, K. S. *Inorg. Chem.* **2000**, *39*, 953.
(84) Aquino, M. A. S.; Lee, F. L.; Gabe, E. J.; Bensiman, C.; Greedan, J. E.; Crutchley, R. J. *J. Am. Chem. Soc.* **1992**, *114*, 5130.
(85) Glöckle, M.; Kaim, W. *Angew. Chem., Int. Ed. Engl.* **1999**, *38*, 3072.
(86) Ung, V. A.; Cargill Thompson, A. M. W.; Bardwell, D. A. Gatteschi, D.; Jeffrey, J. C.; McCleverty, J. A.; Totti, F.; Ward, M. D. *Inorg. Chem.* **1997**, *36*, 3447.

stability of the mixed-valence complex. On the whole, our study showed that the trinuclear Cu^{I}_3 center does not provide efficient conduit for electron delocalization and should be regarded as a poor "conductor". We argued that the low conductivity is due to the disruption of π-conjugation between the terminal Fc groups.

Acknowledgment. J.H.K.Y. thanks The National University of Singapore for financial support. K.Y.W. acknowledges the support from the Hong Kong Polytechnic University. Ms. G. K. Tan (NUS) is thanked for assistance with the X-ray crystal structure determination. Dr. Ng Siu Choon (NUS) is thanked for providing access to the near-infrared absorption spectrophotometer.

Supporting Information Available: Tables of crystallographic data collection parameters, atomic coordinates, and complete listing of bond lengths and bond angles for **1**, **2**·$2CF_3SO_3$·H_2O, and **3**·PF_6 are available free of charge via the Internet at http://pubs.acs.org.

OM010998M